Supplementary Information

Engineering Antimicrobial Peptide Fibril with Feed-Back Degradation of Bacterial-Secreted Enzyme

Fenghua Wang,[a,b‡] Wencheng Xia,[c‡] Mingming Zhang,[c] Rongrong Wu,[a] Xiaolu Song,[a] Yun Hao,[a] Yonghai Feng,[a] Liwei Zhang,[a] Dan Li,[d,e] Wenyan Kang,[f,g] Cong Liu,*[c,g,h] Lei Liu*[a]

*Corresponding author: Cong Liu (liulab@sioc.ac.cn) and Lei Liu (liul@ujs.edu.cn)

1. Materials and methods

1.1 Materials

1,1,1,3,3,3-Hexafluoro-2-propanol (HFIP, 99.0 %, Tokyo Kachina), 1-ethyl-3-(3-dimethylaminopropyl) carbodiimide hydrochloride (EDAC, ≥98.0 %, Sigma), N-hydroxysuccinimide (NHS, 98.0 %, Sigma), 2-Chlorotrityl chloride resin (1.03 mmol/g, Tianjin Nankai, China), Fmoc-protected amino acids (≥95.0 %, Chengdu Chengnuo, China), Tris (hydroxymethyl) aminomethane (Tris base, ≥99.0 %, Aladdin), Brij-35 (OKA) were used as received. O-nitrophenyl-β-D-galactopyranoside (ONPG, ≥98 %), N-Phenyl-1-naphthylamine (NPN, 98.0 %) and gelatinase were purchased from Sigma-Aldrich Co., LLC. Trifluoroacetic acid (TFA, ≥99.5 %), acetonitrile (ACN, ≥99.0 %), piperidine (≥99.0 %), diisopropylethylamine (DIPEA, 99.0 %), methanol (MEOH, ≥99.5 %), formic acid (FA, ≥98.0 %) and all the other AR-grade solvents in this work were purchased from Shanghai Reagent General Factory and used as received. Dichloromethane (DCM),

triethylamine (TEA), tetrahydrofuran (THF) and *N, N*-dimethylformamide (DMF) were dried with CaH_2 and distilled by a general method before use. The HPLC-grade solvent was purchased from Sigma-Aldrich (Shanghai, China). The peptide synthesis was performed at Qiangyao Biotech (Shanghai, China). Peptone, yeast extract and Cell Counting Kit (CCK8) were purchased from Solarbio (Beijing, China). Cellular Ca^{2+} concentration quantitative determination kit (Genmed Scientifics Inc, USA) was used as received. 0.25 % Trypsin / EDTA solution, streptomycin and penicillin were purchased from Gibco BRL (USA). RPMI 1640 medium and fetal bovine serum (FBS) were purchased from HyClone (USA). 96-well coning culture plates were purchased from Coning Company. The mouse fibroblast (L929) cells were bought from Cell Bank/Stem Cell Bank, Chinese Academy of Sciences. The bacteria strain of *Staphylococcus aureus* (*S. aureus*, ATCC 6538), *Escherichia coli* (*E. coli*, ATCC 8739), *Salmonella enteritidis* (*S. enteritidis,* ATCC 14028), *Pseudomonas aeruginosa* (*P. aeruginosa,* ATCC 10145), *Micrococcus luteus* (*M. luteus,* ATCC4698), and *Bacillus subtilis* (*B. subtilis, ATCC9372*) were obtained from China General Microbiological Culture Collection Center.

1.2 Synthesis of peptides

The peptides AP (GLMVGGVVIA), EAP1 (GPLGMRGGVVIA), EAP2 (GPLGMLGGVVIA), EAP3 (GPLGVLGGVVIA), Mel (Ac-GIGAVLKVLTTGLPA LISWIKRKRQQ-NH_2) and EAP2-Mel (GPLGMLGGVVIAGGGGIGAVLKVLTT GLPALISWIKRKRQQ) were synthesized on 2-chlorotrityl chloride polymer resin using a standard Fmoc based solid phase synthesis strategy. The peptides were then cleaved from the resin in DCM solution with 2 % TFA, purified by HPLC, and characterized through ESI-MS and HPLC to determine the peptide sequence and purity.

1.3 Self-assembly and disassembly of peptides AP, EAP1-3

To prevent any preaggregation, peptide powders were first dissolved in HFIP at a final concentration of 10 mg/mL. An appropriate amount of the dissolved peptide solution was dried in a vacuum oven (Jinghong Co., Ltd.). 500 μM and 1 mM peptide solutions were obtained by dissolving peptide in Tris buffer (20 mM Tris·HCl / 50 mM NaCl / 100 mM $CaCl_2$ / 0.05 % Brij 35, pH 7.4), and incubated at 360 rpm on a shaker at 37°C for 24 h. After that, the same amount of gelatinase solution (100 μg/mL, gelatinase was dissolved in the above Tris buffer) was added into 1 mM AP and EAP1-3 solutions respectively, and then incubated at 37℃, 360 rpm for another 72 h. After 24 h incubation, the above samples were characterized by atomic force microscopy imaging (AFM, multimode 8, Bruker), transmission electron microscope (TEM, HT7800, HITACHI), Thioflavin T (ThT) assay (microplate reader, Bio-Tek Synergy H1), circular dichroism spectra (CD, PTC-348W1, JASCO), and fourier transform infrared spectroscopy analysis (FT-IR, Nicolet iS50, Thermo Scientific).

1.4 MD Simulation details

In order to investigate the self-assembly ability of these four peptides (AP and EAP1-3), we used molecular dynamics simulation to study the interaction between the two peptide chains of dimer. Peptide molecules were constructed by Gaussian 09, and obtained by relaxation for 5 ns in an aqueous solution under constant temperature and pressure. In the initial structure of the system, the distance between the COM of the two peptides was 2 nm, and the distance from the periphery of the box was more than 1.5 nm to avoid the influence of period images. The box size of the neutral system is $9 \times 9 \times 9$ nm^3. These four systems were filled with 6842, 6824, 6829 and 6824 water molecules respectively, and ions

are added to balance the charge, and the water molecule was adopted the TIP3P model. After the EM and NPT of the system, a 100 ns simulation was performed, and the data acquisition interval was 1 ns. The NPT (T = 298 K and P = 1 bar) ensemble was applied with the pressure regulated using a Berendsen barostat and temperature-controlled using a velocity-rescale thermostat. The entire simulation was implemented with Gromacs 2020 software, and snapshots were drawn using the Visual Molecular Dynamics (VMD) program.

1.5 Umbrella sampling

The mean force potential (PMF) was calculated using the umbrella sampling algorithm for the most dominant and stable clusters at the end of these four simulations. An external force was applied to the stable structure of the aggregate in the system, and one of the peptide chains was pulled away with 6 nm along the direction away from the centroid, which is defined as the reaction coordinate. Finally, the weighted histogram analysis method (WHAM) was used to conduct umbrella sampling for all trajectories, and the data was processed to draw the PMF curve. The value of ΔG was the difference between the plateau area of the PMF curve and the minimum point of the curve energy.

1.6 Characterization and data analysis of in situ enzyme-responsive disassembly of EAP2 fibrils

10 μL prepared EAP2 fibril solution (diluted to 100 μM with water) was deposited onto freshly cleaved mica and dried. In vitro liquid loading was performed using a liquid cell device, and imaging and micromanipulation were performed in ScanAsyst mode. The disassembled process of EAP2 was observed by AFM (Bruker, Muti-VIII) in liquid gelatinase solution (0.5 mg/mL) using Scanasyst fluid cantilevers with a rated 0.8 Hz

resonate frequency. The peak force frequent was set to 2 kHz during scanning. In situ scanning of EAP2 fibrils during the disassembling process were captured by collecting AFM images every 10 min. All of the recorded AFM images consisted of 512 × 512 pixels. Data were handled by NanoScope Analysis. The disassembling positions of some fibril were marked, and the modulus data of every pixel in the region of growing ends were collected. The lengths of individual fibril were recorded by time. Surface coverage was analyzed through SPIP 6.7.8.

1.7 Enzyme-responsive degradation validation of EAP2 (LC-MS)

The following mixture was prepared: peptide (10 mg/mL), gelatinase (2 U) in buffer (20 mM Tris·HCl / 50 mM NaCl / 100 mM $CaCl_2$ / 0.05 % Brij 35, pH 7.4) with a total volume of 0.5 mL. The peptide residues after exposition for 12 h to gelatinase (37℃, 360 rpm) were analyzed by LC-MS (AB SCIEX API-150EX, USA, acetonitrile (0.1 % TFA) / water (0.1 % TFA) linear gradient from 5 % / 95 % to 60 % / 40 % in 30 min flux 1 mL/min, 220 nm detection).

1.8 Cryo-EM data collection, helical reconstruction and atomic model building of EAP2 fibrils

Cryo-EM sample preparation. EAP2 fibril sample was applied to glow-discharged holey carbon Cu grids (Quantifoil R2/1, 300 mesh), and then plunge frozen in liquid ethane after blotting with filter paper by using Vitrobot Mark IV (Thermo Fisher).

Data collection. The cryo-EM micrographs were collected by a Titan Krios G4 transmission electron microscope (Thermo Fisher) operated at 300 kV with a BioContinuum K3 direct detector (Gatan), using a GIF Quantum energy filter (Gatan) with a slit width of 20 e^-V to remove inelastically scattered electrons. 40 frames per micrograph

were recorded at super-resolution mode in ×105,000 magnification with a pixel size 0.83 Å pixel^{-1}. The total dose was about 55 e^{-}Å^{2} with the exposure time of 2 s, and cryo-EM data collection was performed by EPU software (Thermo Fisher) with a defocus from -1.4 to -2.2 μm.

Imaging processing. Motion correction implement of MotionCorr2[1] was used to correct beam-induced motion of movie frames with dose-weighting. After that, the CTFFIND-4.1.8[2] was applied to estimate the contrast transfer function of motion-corrected images. At last, fibrils were picked manually in RELION3.1.[3]

Helical reconstruction. 58,888 manually picked fibrils from 4,117 micrographs were extracted to segments in the box size of 360 pixels with an inter-box distance of 30.0 Å. Then, these segments were applied to several iterations of two-dimensional (2D) classification with a decreasing in-plane angular sampling rate from 8° to 0.5° and the T = 2 regularization parameter. For two kinds of fibrils separated after 2D classification, the selected particles were used to de novo generate an initial 3D reference by relion_helix_inimodel2d program to perform the following 3D classification (K = 3). Local search of symmetry to optimize the helical twist and rise was carried out after separation of β-strands was shown in order to select the clearest classes. 3D auto-refinement with local optimization of helical parameters was be implemented and contrast transfer function (CTF) refinement was executed in order to improve the resolution of reconstruction map. Finally, the overall resolution of 2 classes of EAP2 fibrils was reported as 2.4 Å and 2.6 Å, respectively, according to the gold-standard Fourier shell correlation (FSC) = 0.143 criteria.

Atomic model building and refinement. Based on the density map after post-processing, the atomic models of 2 classes of EAP2 fibrils were built de novo and improved in COOT.[4] Then, one-layer or two-layer model was generated in Chimera and refined by "real-space refinement" program in PHENIX.[5] Additional details are shown in Table S2.

1.9 Self-assembly and disassembly of peptides EAP2-Mel

The procedures for self-assembly and disassembly of peptides are the same as **Self-assembly and disassembly of peptides AP, EAP1-3**. The apparent morphology and secondary structure of the obtained samples were characterized by AFM, TEM and CD.

1.10 Minimum inhibitory concentration (MIC) determination

For the MIC test in the aerobic condition, *E. coli, S. aureus, S. enteritidis, P. aeruginosa, M. luteus* and *B. subtilis* were cultured in Luria-Bertani (LB) medium under constant shaking at 160 rpm, 37°C to reach the mid-exponential growth phase. The bacterial solution was plated on an agar plate for colony forming unit (CFU) counting. Bacterial suspensions were diluted to approximately 2×10^5 CFU/mL in LB medium. Peptide solutions (EAP2 fibrils, Mel monomer, EAP2-Mel monomer and SANs) at various concentration (320, 160, 80, 40, 20, 10, 5, and 2.5 μM) were prepared in PBS buffer through filter sterilization and exposed under UV light for at least 30 mins. 50 μL of each peptide solution was mixed with 50 μL of bacterial solution in a 96-well plate, and incubated at 37°C, 100 rpm for 16 h, and the optical density (OD) at 600 nm was measured on a plate reader. The MIC was determined at the peptide concentration in which OD reading is below 0.06 and no cloudiness was visible to naked eyes. In addition, the MICs determination of enzyme-responsive disassembled peptides and fibrils were performed by subjecting the products previously treated with gelatinase to the above-mentioned operations.

1.11 Verification of antibacterial mechanism

Bacterial membrane morphology changes and live and dead staining experiment. *E. coli* and *S. aureus* suspensions (~10^7 CFU/mL) were added to prepared peptide solutions (EAP2 fibrils, Mel monomer, EAP2-Mel monomer, SANs) with the final concentration of 80 μM peptide, respectively, co-cultured at 37 °C for 2 h. An equal volume of bacterial suspension in PBS buffer was added as a blank control. Then, the bacterial suspension was centrifuged (5000 rpm, 4 min), washed twice with PBS buffer and resuspended, and an equal volume of 2.5% glutaraldehyde was added and left in a 4 °C refrigerator for 6 h to fix the bacteria appearance. Subsequently, the fixed bacteria were dehydrated with ethanol gradients (30 % × 15 min, 50 % × 15 min, 70 % × 15 min, 85 % × 15 min, 90 % × 15 min, 95% × 15 min, 100 % × 2 × 15 min), and finally, 20 μL of the sample was placed on a silicon wafer, and the bacteria was dried using the critical point method. The samples were placed on carbon tapes, sputter-coated with gold-palladium for SEM imaging. Similarly, LIVE / DEAD (SYTO-9 / PI) staining was performed on the obtained bacterial solution, and it was observed under the Olympus inverted fluorescence microscope (IX73, Japan).

Outer membrane permeability assay. NPN is a widely used fluorescent probe in bio-membrane studies. The fluorescence intensity of NPN in a nonpolar or hydrophobic environment is much stronger than that in aqueous environments, and thus it can be used for indexing the membrane circumstance. In this study, by measuring the fluorescence intensity of NPN in the outer membrane of *E. coli*， EAP2 fibrils, Mel monomer, EAP2-Mel monomer and SANs with the final concentration of 80 μM peptide to increase outer-membrane permeability of Gram-negative bacteria was determined. The cells were cultured to mid-log phase in LB medium and then washed and resuspended in PBS buffer

to an OD600 nm of 0.5. NPN was dissolved in acetone to a final concentration (in cell suspension) of 10 μM. The fluorescence background of the mixture of peptide and NPN was subtracted from all the experimental groups. In the control group, peptides were replaced by PBS. The fluorescence emission intensities were measured with a microplate reader (Bio-Tek Synergy H1, USA) with excitation at 350 nm and emission at 420 nm every 5 min for 1.5 h at 37 °C. The mixture was shaken for 10 s before measuring.

Inner membrane permeability assay. ONPG can be metabolized to ONP by β-galactosidase in the cytoplasm. Therefore, the amount of ONP reflects the level of penetration of the inner membrane. In the experiments, *E. coli* was cultured to mid log phase in LB medium containing 2 % lactose. The cells were then spun down (10,000 rpm, 1 min) and resuspended in PBS (pH 7.4). After washing for three times, the cells were diluted to the concentration with an OD600 nm of 0.05 by PBS containing EAP2 fibrils, Mel monomer, EAP2-Mel monomer and SANs, and the final concentration of the peptide was 80 μM. In the control group, peptides were replaced by PBS. Then, the cells were mixed with ONPG, and the mixtures were added into 96-well plates, in which each well contained cells (100 μL) and ONPG (10 μL). The mixture was shaken for 5 s before measuring. OD420 nm was recorded in the microplate reader every 2 min for 2 h at 37 °C (Bio-Tek Synergy H1, USA)

Bacterial intracellular calcium concentration. *E. coli* and *S. aureus* suspensions (~10^8 CFU/mL) were added to the pre-prepared solutions of EAP2 fibrils, Mel monomer, EAP2-Mel monomer, and SANs, and the final concentration of the peptide was 80 μM. Co-cultured at 37 °C for 2 h. An equal volume of bacterial suspension in PBS buffer was added as a blank control. Then, 1 mL of the bacterial suspension was centrifuged (5000 rpm, 4

min), washed twice with PBS buffer and resuspended. The intracellular calcium ion concentration was determined by a quantitative assay kit for cellular Ca^{2+} concentration (Genmed scientific Inc, USA, catalog number: GMS10152). An equal amount of calcium ion-specific fluorescent probe Fura-2-AM (5 μM) was added to the bacterial solutions of different experimental groups and incubated at 37°C for 2 h. Then, the samples were washed three times with PBS solution to remove excess Fura-2-AM. Fluorescence intensity was measured using a microplate reader (Bio-Tek Synergy H1, USA) with excitation at 340 nm and emission at 380 nm.

1.12 Cytotoxicity measurement

L929 cells (Mouse epithelioid fibroblasts) were seeded onto a 96-well plate at a density of 5×10^3 cells/well and incubated for 24 h at 37 °C in an incubator with 5 % of CO_2. After 24 h, the culture medium was removed. 10 μL of peptide solution at various concentrations (800, 400, 200, 100, 50, 25, and 12.5 μM) was mixed with 90 μL fresh culture medium in a 96-well plate. After another 24 h of incubation, the CCK8 assay was performed to quantify the cell viability by monitoring the UV absorbance at 450 nm. Cell culture without peptides were used as a negative control. All the experiments were performed in six replicates. In addition, the cytotoxicity detection of enzyme-responsive disassembled peptides and fibrils is performed by subjecting the products previously treated with gelatinase to the above-mentioned operations.

1.13 Hemolytic performance verification

Red blood cells (RBCs) were obtained from mice and 4 % of RBCs were prepared in PBS buffer (pH 7.4). 20 μL of peptide solution at various concentrations (1600, 800, 400, 200, 100, 50, and 25 μM) were prepared in PBS buffer (pH 7.4). Peptides were mixed with 180

μL of RBC suspensions in a 1.5 mL Eppendorf tube. The mixtures were incubated at 37 °C for 1 h, followed by centrifugation at 3000 g for 5 min. 100 μL of the supernatant was taken out and transferred to a 96-well plate. Hemoglobin release was determined by measuring the absorbance of the supernatant at 540 nm on a microplate reader (Bio-Tek Synergy H1, USA). RBCs treated with DI water served as positive controls and untreated RBCs served as a negative control group. Each sample was tested in three replicates. The percentage of hemolysis remained is calculated using the following equation: % hemolysis rate = $(A_{peptide}-A_{negative\ control}) / (A_{DI\ water}-A_{negative\ control}) \times 100$.

1.14 Degradation performance of EAP2-Mel fibrils in bacterial culture solution

E. coli (GE-) and *S. aureus* (GE+) were cultured in M9 basal medium to OD=1 (about 10^8 CFU/mL), centrifuged at 10,000 rpm for 5 min, and filtered through a 0.22 μm filter to obtain a cell-removed *E. coli* culture solution (ECS) and *S. aureus* culture solution (SCS), which were mixed with pre-prepared self-assembled 720 μM self-assembled antibacterial fibrils (SANs) in a ratio of 3:1, in which PBS buffer and M9 basal medium were used as control. Next, the secondary structure changes of peptide were detected by ThT fluorescence method. Specifically, a total of 200 μL sample solution composed of solvent, peptide solution and 1 mM thioflavin T solution was added into a 96-well plate for the final measurement, with the volume ratio of peptide reaction solution and 1 mM thioflavin T solution was 3:1. The fluorescence was recorded by using multifunctional microplate reader (Bio-Tek Synergy H1, USA) with excitation at 450 nm and emission at 470-600 nm. Subsequently, the same amount of ThT fluorescence test solution (50 μL) was taken and dried in a 48-well plate, and observed under a fluorescent inverted microscope (IX73,

Japan). All the measurements were repeated in triplicate and averaged the intensity value of every sample.

2. Figures

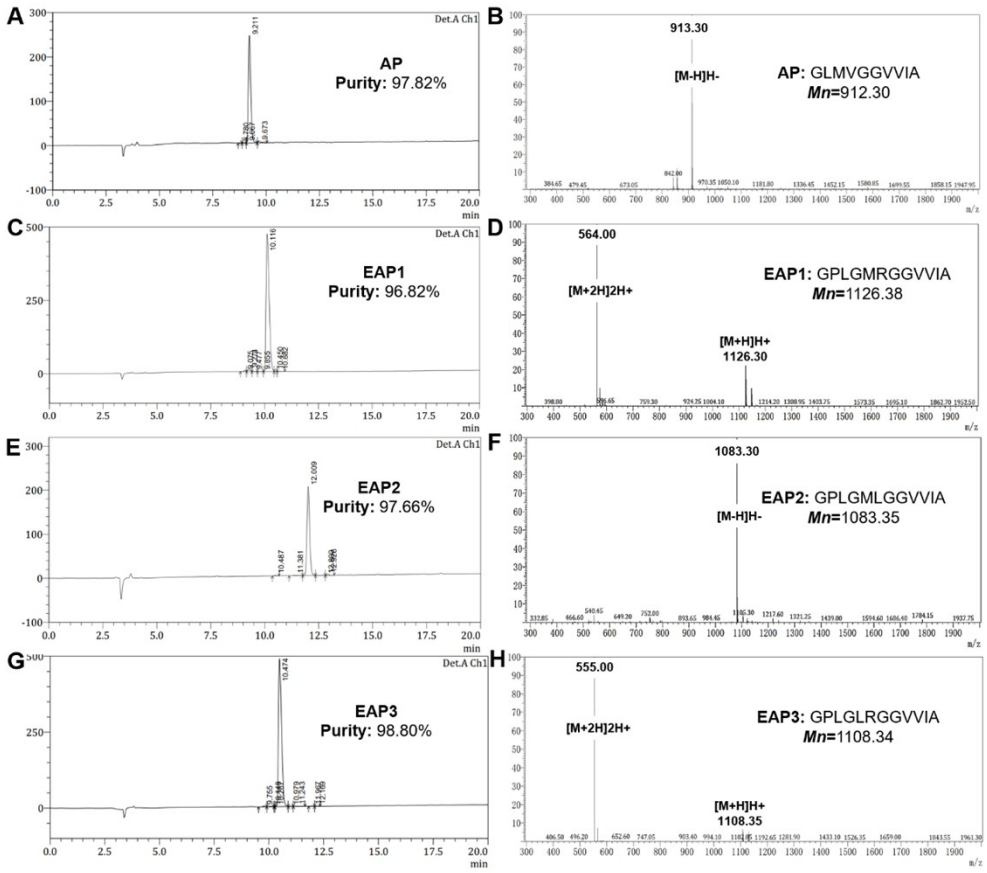

Figure S1. HPLC analysis, molecular weight and ESI mass spectrum of the peptide AP, and EAP1-EAP3.

All the peptides (AP, EAP1-EAP3) were prepared by solid-phase synthesis, and purified by high performance liquid chromatography (HPLC) and identified by electrospray ionization mass spectrometry (ESI-MS) (Figure S1).

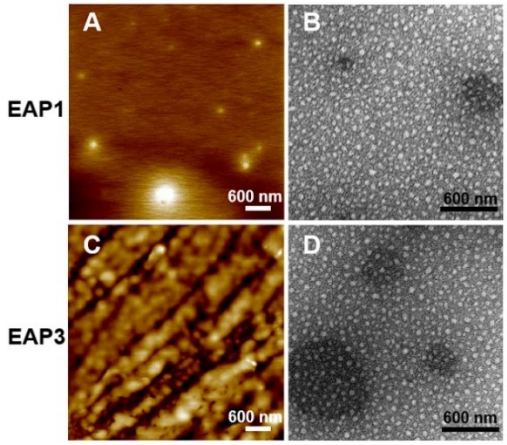

Figure S2. AFM and TEM characterization of the self-assembled morphologies of EAP1 and EAP3 (500 μM) in Tris buffer.

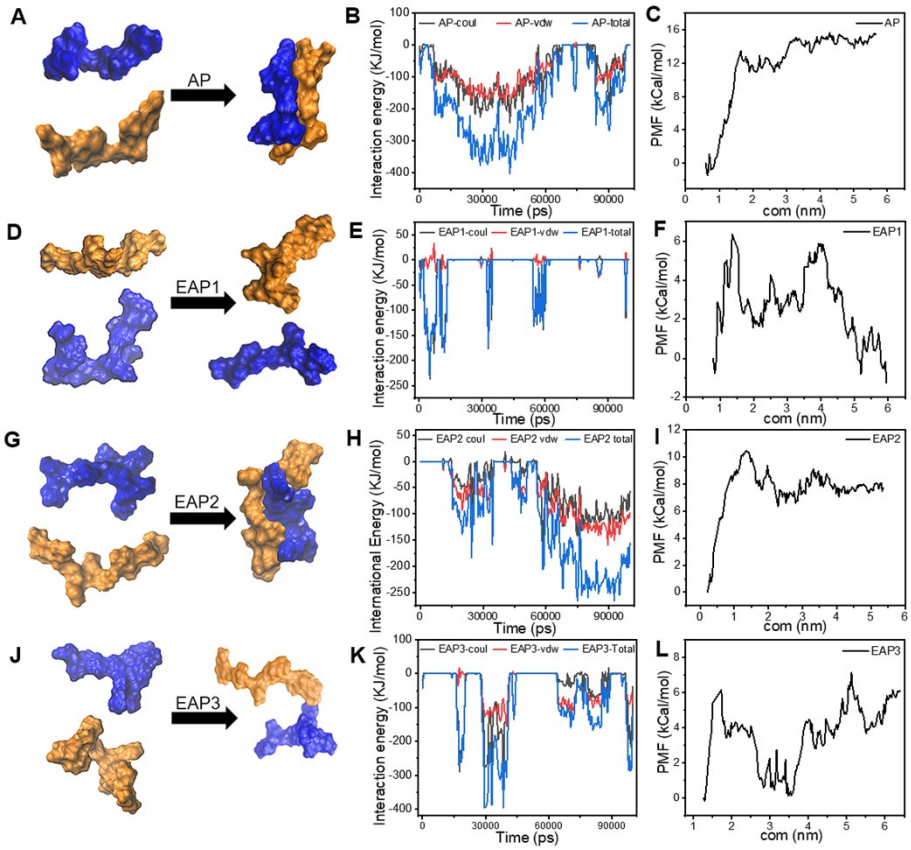

Figure S3. The initial and the finial conformation changes of these four peptides in molecular dynamic simulations, the interaction energy between the two chains of the peptide dimer as a function of time, and the PMF plots of umbrella sampling simulation of peptide AP (A-C), EAP1 (D-F), EAP2 (G-I) and EAP3 (J-L).

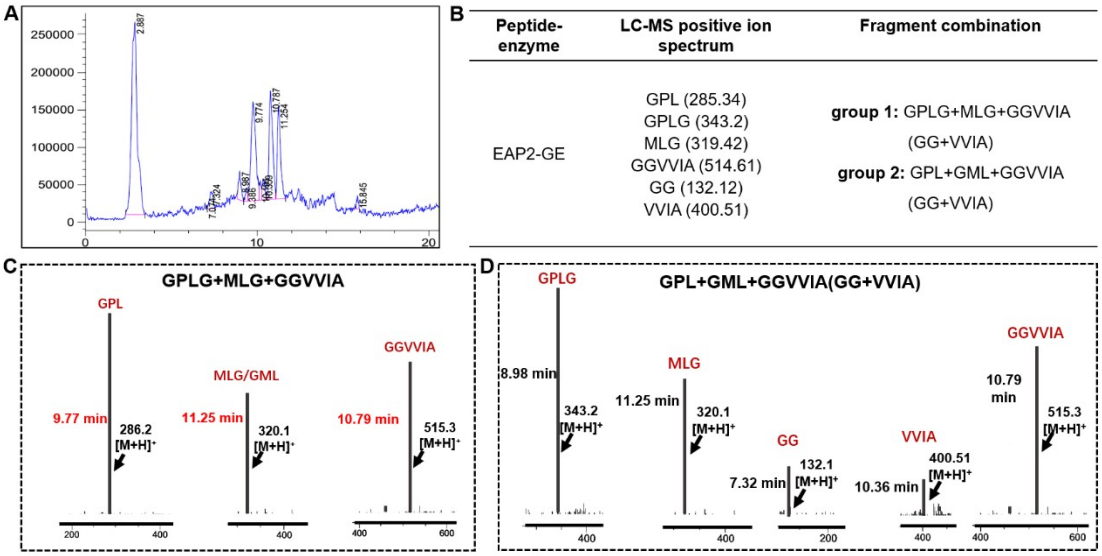

Figure S4. Characterizations of LC-MS for gelatinase responsive peptide of EAP2 (A). (B-D) The amino acid sequence of EAP2 treated by gelatinase was obtained by LC-MS analysis.

There are two compositions of degraded short peptides, the first group (group 1) was composed of Gly-Pro-Leu-Gly (343.2 $[M+H]^+$, 8.98 min), Met-Leu-Gly (320.1 $[M+H]^+$, 11.25 min) and Gly-Gly-Val-Val-Ile-Ala (515.3 $[M+H]^+$, 10.79 min), and the second one (group 2) was composed of Gly-Pro-Leu (285.34 $[M+H]^+$, 9.77 min), Gly-Met-Leu (320.1 $[M+H]^+$, 11.25 min) , Gly-Gly-Val-Val-Ile-Ala (515.3 $[M+H]^+$, 10.79 min), Gly-Gly (132.1 $[M+H]^+$, 7.32 min) and Val-Val-Ile-Aal (400.51 $[M+H]^+$, 10.36 min). The above results showed that EAP2 could be degraded into short fragments in the presence of gelatinase, which was the essence of degradation of peptide fibrils. The short peptide fragment degraded could not self-assemble into the fibrils as before. The above results showed that gelatinase targeted EAP2-specific enzyme responsive substrate sequences (PLGMLG) and could degrade them into short fragments (group 1). In addition, since the amino acid sequence of PLG and GPL, GML and MLG in EAP2 were only differences in the order of amino acid, gelatinase might target and cleaved the short peptides of similar sequences, thereby degrading EAP2 into short peptide fragments in the second group.

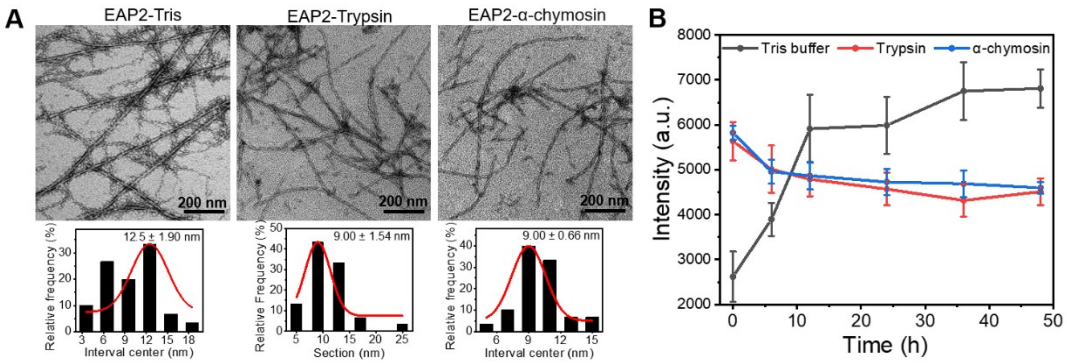

Figure S5. Stability verification of EAP2 fibrils. (A) TEM characterization of the EAP2 (500 μM) fibrils in Tris buffer, trypsin and α - chymotrypsin solution (50 μg/mL). (B) Fluorescence kinetics of thioflavin T (ThT) interacted with EAP2 fibrils.

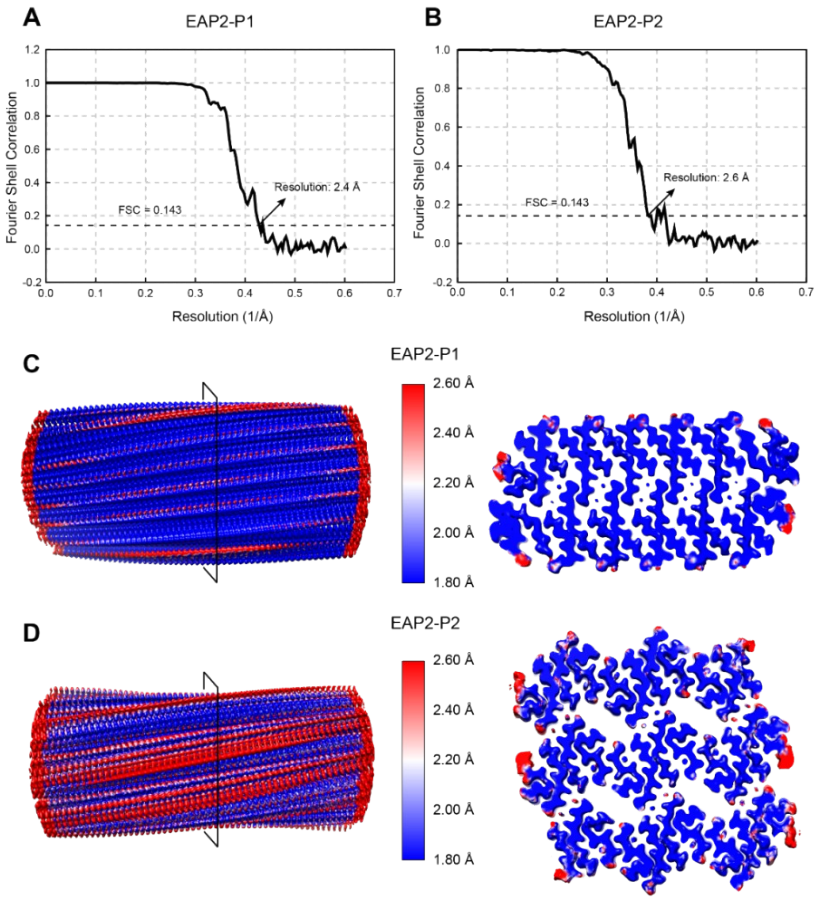

Figure S6. (A-B) Gold-standard Fourier shell correlation (FSC) curves of EAP2-P1 and EAP2-P2. (C-D) Local resolution estimations of the density maps of EAP2-P1 and EAP2-P2.

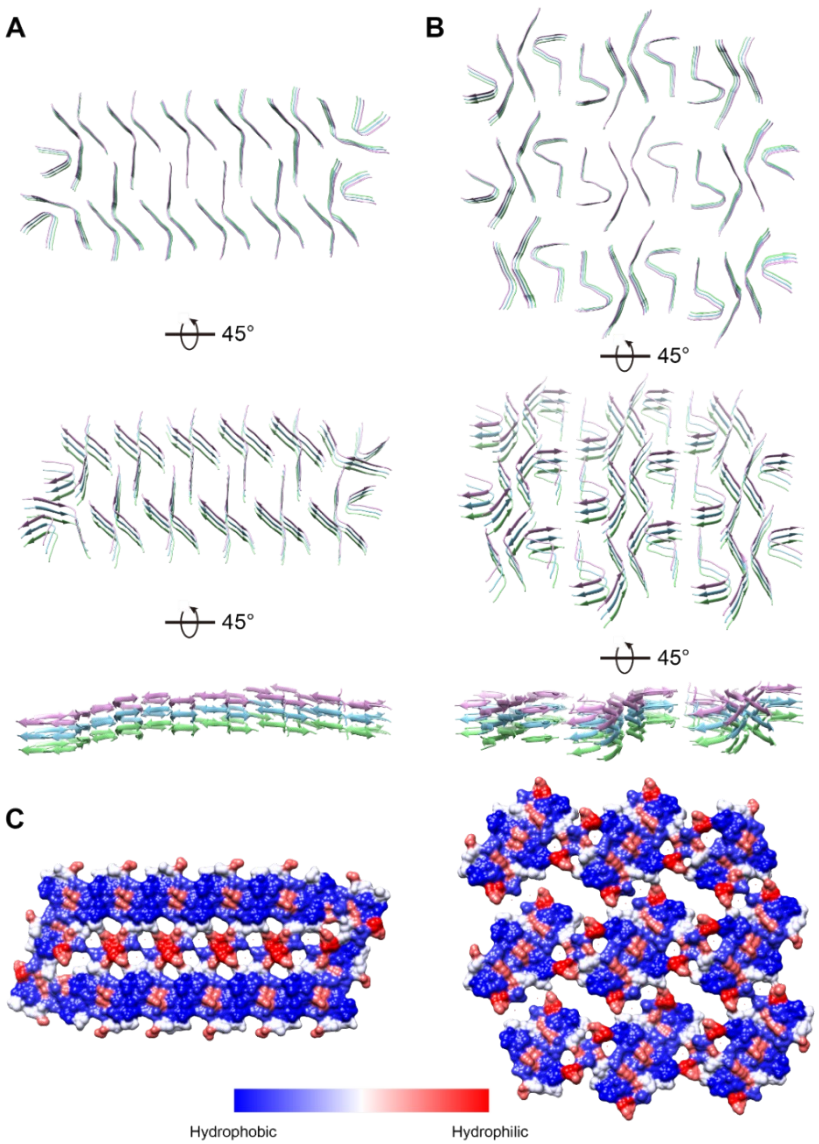

Figure S7. (A-B) Views of three layers of EAP2 fibrils are shown in cartoon. (C) The surfaces of one layer of EAP2-P1 (left) and EAP2-P2 (right) are shown according to the hydrophobicity of the residues.

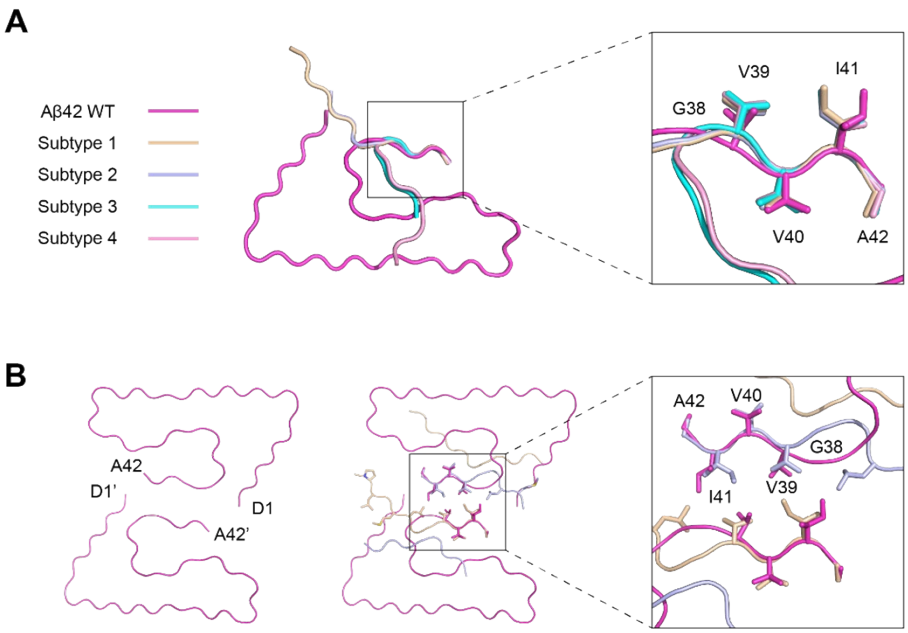

Figure S8. (A) Structure comparison of Aβ42 WT (PDB: 5OQV) subunit and 4 subtypes with zoom-in view in the right. (B) Structure comparison of Aβ42 WT (PDB: 5OQV) and dimer 1 with zoom-in view in the right.

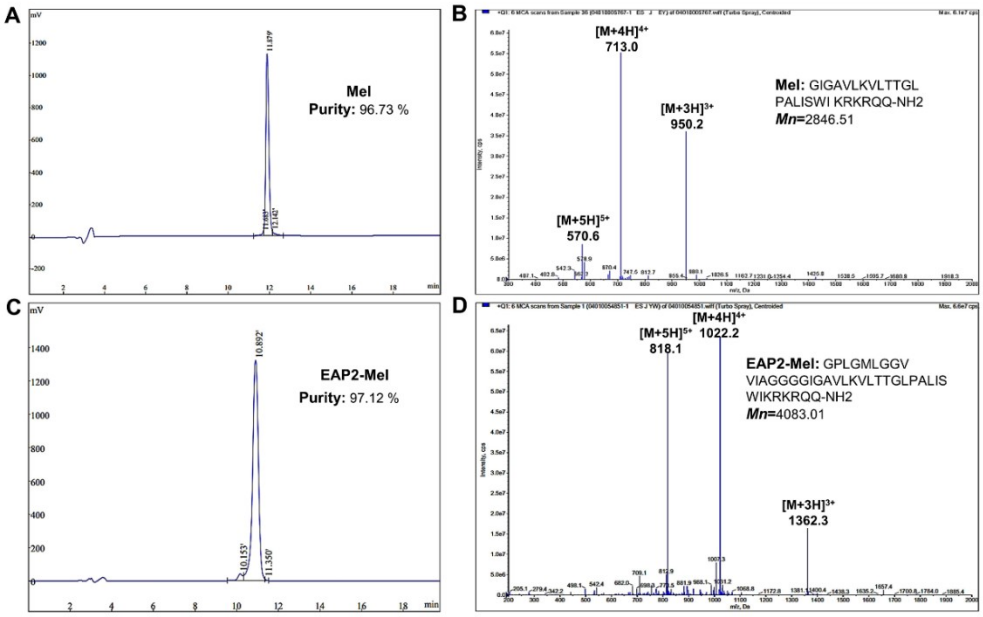

Figure S9. HPLC and ESI mass spectrum of (A-B) Mel; (C-D) EAP2-Mel.

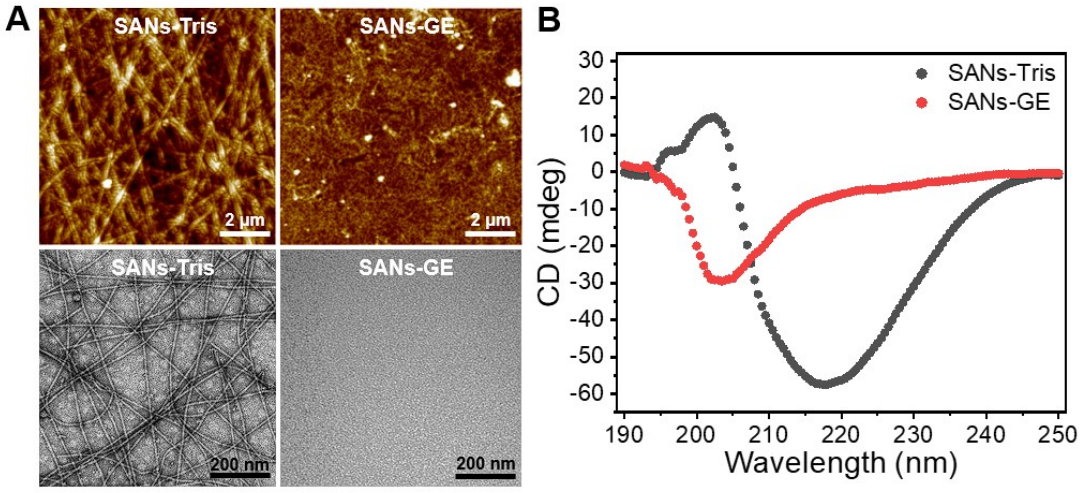

Figure S10. AFM, TEM and CD characterization of SANs (Tris) and 48 h disassembly in gelatinase solution (GE).

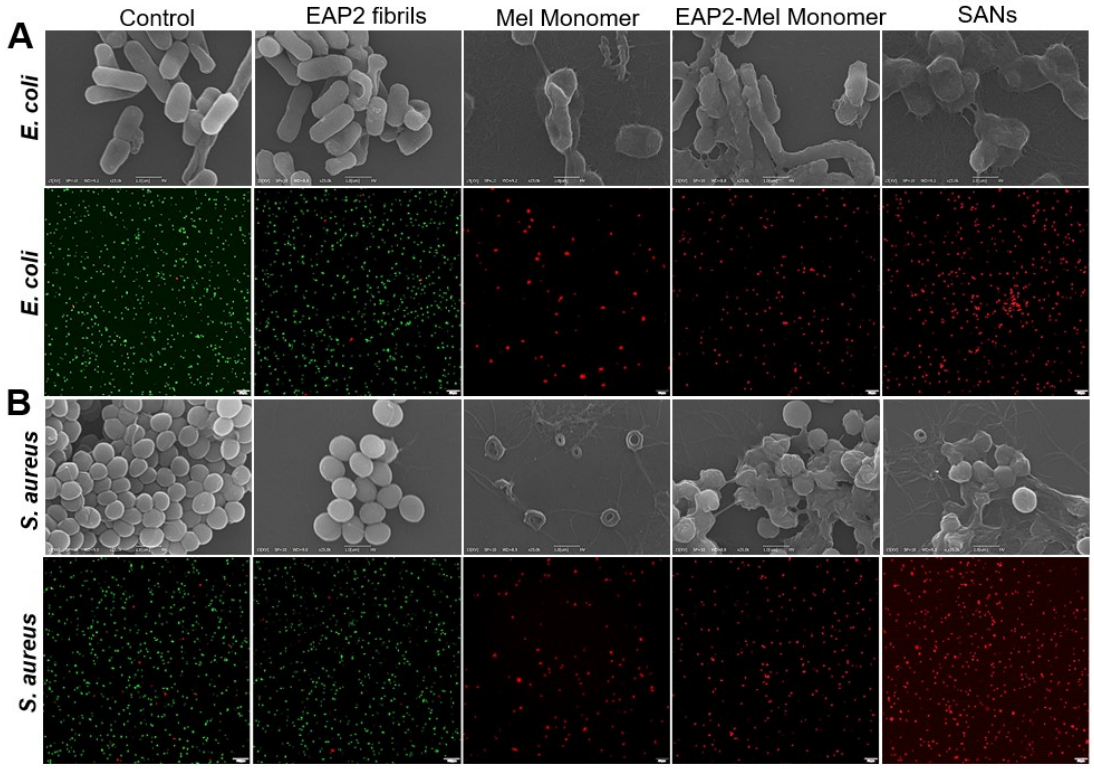

Figure S11. (A-B) Bacterial membrane morphology changes and live and dead staining experiments of bacteria E. coli and S. aureus after treatment with PBS (control), EAP2 fibrils, Mel monomer, EAP2-Mel monomer, and SANs for 2 h.

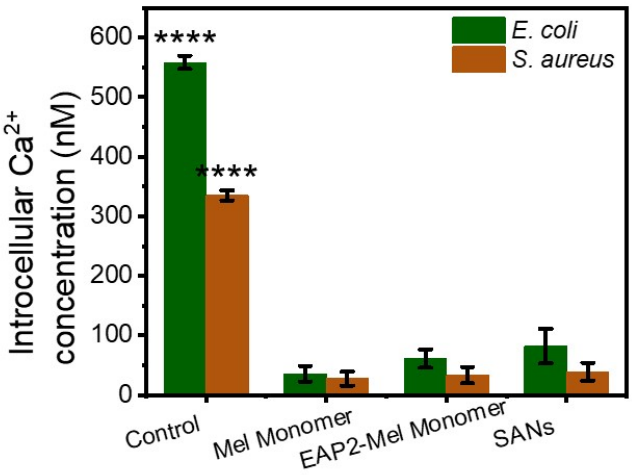

Figure S12. The intracellular calcium concentration of bacteria E. coli and S. aureus with the treatment of EAP2 fibrils, Mel monomer, EAP2-Mel monomer, and SANs. One-way analysis of variance (ANOVA), $P < 0.0001$.

Table S1. Summary of morphology, height and width analysis results of peptides AP and EAP1-3 self-assembled in Tris buffer and unassembled in gelatinase buffer (GE).

Peptide	Tris buffer (Tris)			Gelatinase buffer (GE)		
	Morphology	Height (nm)	Width (nm)	Morphology	Height	Width (nm)
AP	β-Sheet	3.95 ± 1.68	20.5 ± 4.03	β-Sheet	None	25 ± 10.58
EAP1	None	None	None	None	None	None
EAP2	Twist β-Sheet	12.34 ± 1.05	11.5 ± 6.87	None	None	None
EAP3	None	None	None	None	None	None

Table S2. Cryo-EM structure determination and statistics of model building.

Data collection and processing	**EAP2 polymorph 1** (EMD-34392) (PDB 8GZ8)	**EAP2 polymorph 2** (EMD-34393) (PDB 8GZ9)
Data Collection		
Magnification	105,000	105,000
Pixel size (Å)	0.83	0.83
Defocus Range (μm)	-1.4 to -2.2	-1.4 to -2.2
Voltage (kV)	300	300
Camera	BioContinuum K3	BioContinuum K3
Microscope	Krios G4	Krios G4
Exposure time (s/frame)	0.05	0.05
Number of frames	40	40
Total dose ($e^-/Å^2$)	55	55
Reconstruction		
Micrographs	4,117	4,117
Manually picked fibrils	58,888	58,888
Box size (pixel)	360	360
Inter-box distance (Å)	30	30
Initial particle images (no.)	733,119	92,529
Final particle images (no.)	279,380	53,633
Resolution (Å)	2.35	2.62
Map sharpening B-factor ($Å^2$)	-91.5043	-79.4562
Helical rise (Å)	179.539	179.548
Helical twist (°)	2.407	2.404
Atomic model		
Non-hydrogen atoms	3,336	2,426
Protein residues	540	390
Ligands	0	0
r.m.s.d. Bond lengths	0.005	0.003
r.m.s.d. Bond angles	0.730	0.686
All-atom clash score	6.32	1.93
Rotamer outliers	0 %	0 %
Ramachandran Outliers	0 %	0 %
Ramachandran Allowed	0.46 %	0.31 %
Ramachandran Favored	99.54 %	99.69 %

3. SI references

1. S. Q. Zheng, E. Palovcak, J. P. Armache, K. A. Verba, Y. Cheng and D. A. Agard, MotionCor2: anisotropic correction of beam-induced motion for improved cryo-electron microscopy, *Nat. Methods*, 2017, **14**, 331-332.
2. A. Rohou and N. Grigorieff, CTFFIND4: Fast and accurate defocus estimation from electron micrographs, *J. Struct. Biol.*, 2015, **192**, 216-221.
3. S. H. W. Scheres, Amyloid structure determination in RELION-3.1, *Acta Crystallogr. D Struct. Biol.*, 2020, **76**, 94-101.
4. P. Emsley, B. Lohkamp, W. G. Scott and K. Cowtan, Features and development of Coot, *Acta Crystallogr. D Biol. Crystallogr.*, 2010, **66**, 486-501.
5. P. D. Adams, P. V. Afonine, G. Bunkóczi, V. B. Chen, I. W. Davis, N. Echols, J. J. Headd, L. W. Hung, G. J. Kapral, R. W. Grosse-Kunstleve, A. J. McCoy, N. W. Moriarty, R. Oeffner, R. J. Read, D. C. Richardson, J. S. Richardson, T. C. Terwilliger and P. H. Zwart, PHENIX: a comprehensive Python-based system for macromolecular structure solution, *Acta Crystallogr. D*, 2010, **66**, 213-221.